Simulation of Fluid Flow in DI Diesel Engine for Different Bowl Configurations

Dr. A. Sreekanth Gowd
Principal, Bheema Institute of Technology & Science,
Adoni, Kurnool (Dist.), A.P, India.

Prof. K. Hemachandra Reddy
Registrar, JNT University Anantapur,
Anantapuramu, A.P, India

Dr. M. Srinivasa Reddy
Technical Assistant, JNTUA College of Engineering Anantapur,
Anantapuramu, A.P, India

***Abstract*— Understanding in-cylinder gas dynamics by conducting experiments is rather difficult. Every parameter, such as piston shape, injector inclination and mixing process has to be carefully examined. For this purpose numerical simulation techniques are being used to predict in-cylinder fluid behavior. STAR-CD a general purpose finite volume CFD code is used. The STAR-CD (es-ICE) also provides an automated IC Engine mesh motion description methodology.**

Detailed investigations have been carried out with regard to the dynamic behavior of in-cylinder fluid motion in a single cylinder two valve DI Diesel engine with three different piston bowls viz., Mexican-hat Bowl, Hemispherical Bowl and Double swirl combustion Bowl. Study and comparison are done for different parameters like pressure, TKE and swirl for these geometries. The validation of the code is done by comparing the predicted global parameters with the experimental data available in the literature. Results are compared with three bowl configurations for different parameters and it is observed that Double Swirl Combustion Bowl gives the best for the engine under consideration.
Keywords*— *Swirl ratio, Turbulent kinetic energy, Double swirl combustion bowl, Turbulence, Fuel injection.

I. Introduction

Increasing environmental concerns and legislated emission standards have lead to the necessity of both conventional and unconventional means for reducing soot and NO_x emissions in diesel engines. The need for faster, cleaner, and more fuel-efficient engines is from society's desires and regulatory mandates. This poses a very complex problem for engine designers, since many of these goals are competing. The process is further complicated because the in-cylinder fluid dynamics is still not fully understood. In the pursuit of these goals, it is necessary to have as a thorough understanding of engine phenomena.

Direct injection diesel engines are widely used in industrial applications and as vehicular power sources and compact designs are used in passenger cars. Environment concerns have led to stringent emission regulations for diesel engines. Incomplete combustion is mainly responsible for the emissions, and better mixture formation would be the best way to improve the combustion and emission quality. Effective spray mixing process in a DI diesel engine is the most important factor to improve the engine performance such as power, exhaust emissions, fuel consumption are affected drastically by the shape and the arrangement of the combustion chamber. Also, the in-cylinder fluid motion and thermodynamic parameters such as temperature and pressure greatly influence fuel-air mixing.

II. Previous Work

Over the past one and half decades many models have been reported for two and three dimensional engine flows with fuel spray and combustion [1-7]. Much progress has been made in IC engine model development in recent years. The development is rapid in the last five years with the advent of high-speed computational facilities and experimental methods that provide a base for verifying the model computations. Because of the complications in the modeling of the ignition and combustion processes in DI diesel engines, it is not yet possible to model all the phenomena in a comprehensive manner. Even the most sophisticated fluid dynamic based codes now available are not able to reveal complete details of the engine process.

III. Theoretical Model

The gas flow within the cylinder is extremely complex and three-dimensional. They are unsteady and turbulent in nature due to the reciprocating piston movement. In the present work a time marching three-dimensional, finite difference program is used to steady the fluid flow. This program solves three-dimensional differential equations of conservation of mass, momentum, energy and species concentrations. To get the solution for a continuum problem such as flow field inside the engine cylinder, the continuum is represented by a finite number of discretization. This means to divide the region of interest into a number of small cells. These cells form a mesh, which serves as a framework for constructing finite volume approximations to the governing partial differential equations. The time variable is similarly discretized into a sequence of small time intervals called time steps and a transient solution is marched out in time. The following section presents the basic governing equations.

Governing Equations:

The governing equations are written in vector notations. The unit vectors in the x,y, and z, directions are denoted by i, j and k respectively. The position vector x is denoted by

$$x = xi + yj + zk \qquad -----(1)$$

The vector operator ∇ is given by

$$\nabla = i\frac{\partial}{\partial x} + j\frac{\partial}{\partial y} + k\frac{\partial}{\partial z} \qquad -----(2)$$

and the fluid velocity vector **u** is given by

$$u = u(x,y,z,t)i + v(x,y,z,t)j + w(x,y,z,t)k ---3$$

Where 't' is the time. Here $x \neq |x|$ and $u \neq |u|$

The program solves the equations of motion for fluid along with the equations for spray droplets and chemical kinetics.

IV. Boundary Conditions

Temperature and velocity boundary conditions are required to calculate the flow field computational domain. In this work the law of the wall boundary condition is considered to resolve boundary layer near the solid walls while calculating velocities as shown below.

a) When the wall is flat the components of tangential velocity are calculated.
b) When the wall is having curvature is one direction, the component of tangential velocity in the direction of curvature is set to zero and the other component in the direction of no curvature is set equal to the next closest corner(but not on the wall).
c) When the wall is curved in both principal directions (the case of hemispherical bowl) both components of tangential velocity are set to zero.

The normal velocity is always set equal to the velocity of the corresponding wall.

In the present work an attempt is made to investigate the dynamic behavior of in-cylinder fluid motion in a single cylinder DI Diesel engine with different piston bowls viz; (Hemispherical bowl, Mexican-hat and double swirl combustion chamber). Fluid flow behavior in the combustion chamber is predicted using the scheme STAR-CD. The ECFM-3Z combustion model has been invoked to analyze combustion for n-Dodecane liquid fuel. An attempt is made to compare the capabilities of two turbulence models viz; 1) k-ε / High Reynolds number, 2) k-ε /Quadratic/ high-Reynolds number.

V. Mesh Generation for Sector

Only the sector of engine domain has been considered to simulate combustion process. The combustion process simulated between the piston positions 40^0 before TDC (680^0) and 80^0 after TDC (800^0). 120^0 crank angle variation only is considered to minimize the computational time and computer storage requirements. During this crank angle period both the inlet and exhaust valves will be in closed position. Hence, the effect of valves is not considered. 45^0 sectors considered for the analysis.

The simulation requires a moving mesh and boundary algorithm embedded into the STAR-CD programme. The moving mesh and boundary algorithm for this engine model has been developed inside STAR-CD by declaring the events for each time step and then activating the grid in order to move the mesh. The concept of moving mesh is that the cell is squeezed to zero volume over one time step, with all its contents (pressure, temperature, mass, momentum, enthalpy, etc.) being expelled into the neighboring cells. Hence, conservation is satisfied exactly even with removal of any cell layer. On the other hand, when the cell layers are added, they grow from zero size to their full volume, absorbing the conserved variables through their faces.

VI. Analysis Setup

Apply initial and boundary condition like in-cylinder pressure, temperature, swirl ratio and temperatures of cylinder wall, cylinder dome and piston crown at that particular crank angle position. For multi phase treatment Lagrangian multi phase is used. Locate the injector location by creating the coordinate at that point. The z-direction shows the axis of injector. Select the required turbulence model for the analysis. For the problem setup the time domain is taken as transient and the density properties are set to Ideal. For the momentum and turbulence the differencing scheme MARS is used. Under relaxation for pressure correction is set to 0.3.

The fuel considered for the analysis is n-Dodecane with cetane number 60. The properties of the fuel considered for the analysis is given in Table 5.1. The standard model is used for momentum transfer, mass transfer and heat transfer, Reitz model is used for droplet breakup, Bai model is used for droplet-wall interaction. For fuel injection Huh atomization model is use.

VII. Results and Discussion

1) *Validation of Code with Experimental Results:*

It is important to validate the results obtained with the code to ascertain the accuracy of prediction. The effort made is to validate the code by comparing the predicted pressure Vs crank angle curve and heat release rate curve with the experimental p-θ and heat release rate curves published by Tree and faster. The test engine considered by Tree and faster has Mexican hat bowl and the fuel injection starts at 22.5^0 bTDC and end at 10.5^0 aTDC. The computations are performed for the engine with the same specifications and engine geometry so that the comparisons is justified.

Predictive capability of any CFD code, particularly when applied to the complex fluid dynamic problems such as in-cylinder flows in diesel engines, depends on the turbulence models employed. The predictions are carried out by employing k-ε / High Reynolds number (k-ε-high) and k-ε /Quadratic/ high-Reynolds number (k-ε-quad) turbulence models. These models have been identified after careful review of the literature.

The global in-cylinder pressures and heat release rates are predicted for the engine specifications given in Table.1. The predicted global pressure variations and heat release rate with crank angle are compared with those taken from literature[7].

Table.1 Engine Specification for Validation of Code

Engine Specifications	
Bore	13.97 cm
Stroke	15.24 cm
Connecting rod length	30.48 cm
Displacement	2340 cm^3
Compression ratio	15.5
Engine speed	1300 rpm
Number of orifices	8
Orifice diameter	0.2 mm
Spray angle	72^0
Type of fuel	n-dodecane

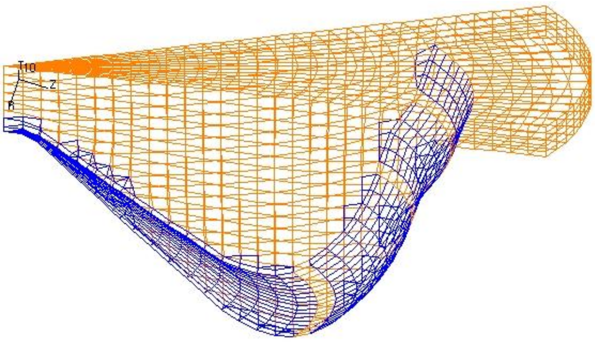

Fig.1 Prospective view of the geometry with at top dead centre

2) Comparison between experimental and predicted pressure histories:

The comparison of the measured and computed pressure histories the two turbulence models viz. k-ε-high turbulence model and k-ε-quad turbulence model is shown in Fig.2. The variation of in-cylinder pressure with crank angle is presented during compression and expansion strokes. The pressure variation is studied from 40^0 bTDC in compression stroke to 80^0 aTDC in expansion stroke. A smooth pressure rise due to compression is noticed from 40^0 bTDC to 22.5^0 bTDC during compression stroke. During this period the pressure rise with both turbulence models is noticed to be almost same and found to increase from 20 bar to 38 bar. After 10^0 bTDC (after the fuel injection) the in-cylinder pressures predicted with the two turbulence models, are not almost same. The k-ε-quad turbulence model is found to predict lower pressures then that of k-ε-high turbulence model. The in-cylinder pressure curve for k-ε-high turbulence model is almost matching with experimental results and with k-ε-quad turbulence model peak pressures are lower in compression to the experimental values. The experimental peak pressure is slightly lower than that of k-ε-high turbulence model. However they are comparable. The peak pressures noticed are 118 bar for k-ε-high turbulence model and 115 bar for k-ε-quad turbulence model. 20^0 aTDC in the expansion stroke all these curves are following same path. Finally the experimental values are closely matching with k-ε-high turbulence model. The predictions made with k-ε-high turbulence model is found to be closer to the experimental values and therefore this model is used for future predictions.

3) Comparison between Experimental and Predicted Heat Release Rate Variation with Crank Angle:

Variation of heat release rate with crank angles predicted with the two turbulence models and the corresponding experimental results are shown in Fig.3. The heat release in the combustion chamber is due to the combustion of fuel. Heat releases are noticed to be similar between 20^0 bTDC to 15^0 bTDC in all the cases. This is mainly due to small quantity of fuel participating in combustion reaction. Sharp rise in heat release rate is noticed in these cases at 50 aTDC indicating bulk of the fuel participating in the combustion. The heat release rate is high with k-ε-high turbulence model as compared to that of experimental values and with k-ε-quad turbulence model predictions. The peak heat release rates are observed at 15^0 aTDC in all the cases. The peak heat release rate is found to be 215 Joule/degree with k-ε-high turbulence model and 205 Joule/degree with k-ε-quad turbulence model. The heat release rates with k-ε-high turbulence model are closer to the experimental values.

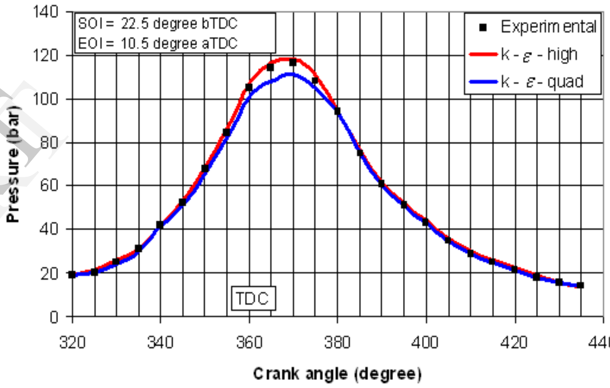

Fig.2 Comparison of Experimental and Predicted p-θ Curves

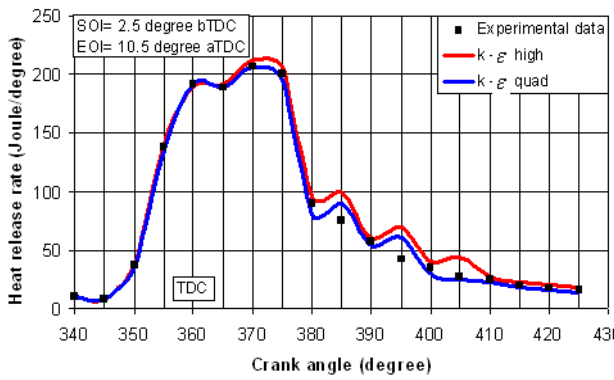

Fig.3 Comparison of Experimental and Predicted Heat Release Rates

From the above discussions it is concluded that the predicted capability of k-ε-high Reynolds number turbulence model is comparatively better than the k-ε-quad turbulence model and is closer to the experimental values. Hence, the k-ε-high Reynolds turbulence model is used in the rest of the analysis presented in the subsequent sessions.

4) Results and Discussion for Different Combustion Chamber Configurations:

In spite of the capabilities of most comprehensive CFD codes, they cannot entirely predict the complete details due to complex in-cylinder flow dynamics. The important aspect in presentation of the results is to process, organise and present the huge data generated by the code. Therefore, it is necessary to present this information in a comprehensive form. In order to study the influences of combustion chamber shape on the fluid flow near TDC, CFD calculations for the compression and expansion stroke have been performed in a single cylinder DI Diesel engine with different piston bowl geometries viz; Hemispherical bowl, Mexican hat bowl and Double swirl combustion bowl.

Table.2 Gives the Specifications of the Engine Under Consideration.

Bore	87.5mm
Stroke	110 mm
Connecting rod length	232 mm
Piston bowl configurations	Hemispherical bowl (HSB) Mexican hat bowl (MHB) and Double swirl combustion bowl (DSCB)
Engine speed	1500 rpm
Initial swirl ratio	2
Initial charge temperature	583 K
Fuel	Normal Decane
Tilt of injector	13^0 to horizontal
Inflow temperature of fuel droplets	310 K
Starts of injection	5.25^0 bTDC
End of injection	2.65^0 aTDC
Mass of fuel injected	as per Fig.4

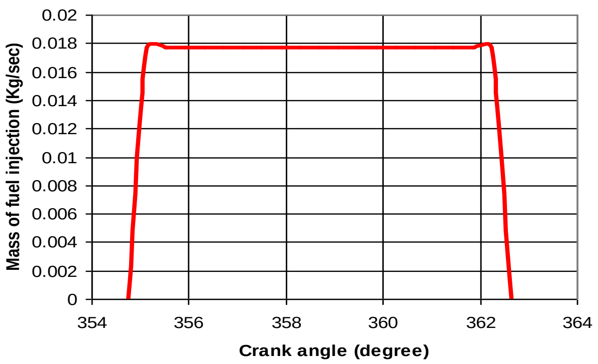

Fig.4 Mass of Fuel Injection Vs Crank Angle

5) Presentation of Result:

A finite volume commercial program (STAR-CD) has been used to solve the discretised Navier-Stokes equations. The k-ε turbulence model for high Reynolds number with standard wall function is used for the analysis. The program is based on the pressure-correlation method and uses the PISO algorithm. The first up-wind differencing scheme (UD) is used for the momentum, energy and turbulent equations. The temporal discretisation is implicit, with variable time step depending on the stage of the cycle. In the present work fluid dynamic analysis which has been carried out includes in-cylinder fluid dynamics during compression, fuel spray, fuel evaporation, combustion and expansion of gases during expansion stroke. In view of constraints in computer memory and storage, the fluid behavior is predicted for a part of compression and expansion strokes.

The calculations begin at 40^0 bTDC of the compression stroke and finish 80^0 aTDC of expansion stroke. The initial values for pressure and temperature at 40^0 bTDC are prescribed as 9.87 bar and 583 K, (based on thermodynamic analysis) with both variables considered as homogeneous in the whole domain. Constant temperature boundary conditions were assigned separately for the combustion dome, piston crown and cylinder wall regions. The temperature on each of these walls depends on the mean piston speed of the engine. The fuel injector is located at (1.5, 0, -1.3) from cylinder axis co-ordinate and the injector angle is 13 degree anticlockwise from horizontal.

The flow field is presented in the form of velocity vectors in the xz-plane at selected crank angles. Eight different crank angle positions that are selected for presentation during compression stroke which include details before and after fuel injection since the fuel injection starts at 5.25^0 bTDC and ends at 2.65^0 aTDC. The starting crank angle position is 38^0 bTDC to TDC. The flow field at 6^0 bTDC position provides information regarding the in-cylinder fluid flow just before fuel injection. The three crank angle positions that are considered during the expansion stroke reveal the information regarding the behavior of fluid flow after combustion.

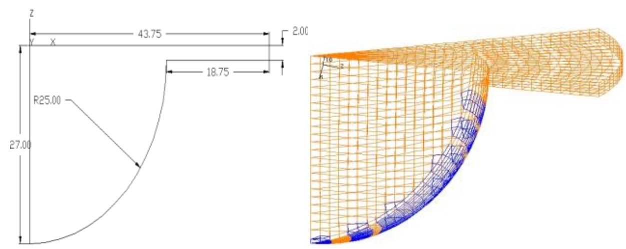

Hemispherical Bowl (HSB)

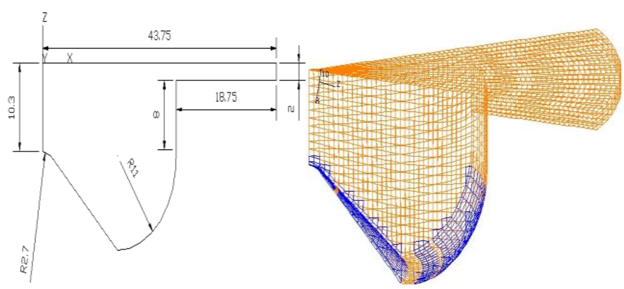

Mexican Hat Bowl (MHB)

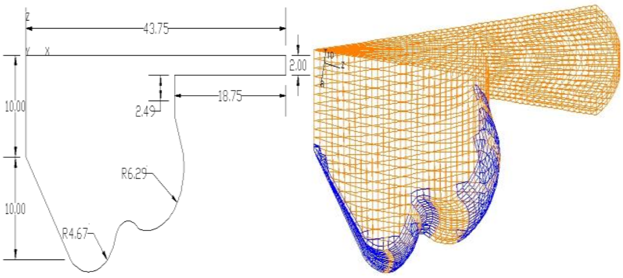

Double Swirl Combustion bowl (DSCB)

Fig. 5 Piston Bowl Geometries & Pictorial View of Computational Mesh for 45^0 Sectors at TDC

6) Effect of Piston BowlConfiguration:

The combustion chamber geometry significantly influences the in-cylinder fluid dynamics, fuel-air mixing and combustion characteristics. It is therefore important to study the effect of piston-bowl configuration on these characteristics. An attempt is made to study the effect of bowl configuration on the fluid flow. The three bowl configurations considered for the analysis are (i) the popular hemispherical bowl (HSB) (ii) Mexican hat bowl (MHB) and (iii) Double swirl combustion bowl (DSCB). The details of these bowl geometries are given in Fig.6.5. The bowl dimensions are selected in such a way that the bowl lip diameter and volume of combustion chamber remains same in all the three cases. Considering the symmetry, computations have been carried out on a 45^0 sector, which includes the cylinder and piston bowl. The number of cells in the sector varies from 66,368 (2,192 Tetrahedral cells and 64,176 Hexahedral cells) at BDC to 7,104 at TDC for HSB. The number of cells in case of MHB varies from 75,024 (1,520 Tetrahedral cells and 73,504 Hexahedral cells) at BDC to 12,804 at TDC. DSCB sector has highest number of cells compared to HSB and MHB. It has 90,736 (2,176 Tetrahedral cells and 88,528 Hexahedral cells) at BDC to 11,024 at TDC. Coarse mesh type is preferred above the piston and fine mesh is used in the bowl region because most of the flow field action takes place in the bowl.

At 20^0 bTDC (Fig.6) the maximum velocities are noticed at the bowl lip in all the three cases. At this stage the maximum velocities are 8.97 m/s, 9.758 m/s and 9.38 m/s in HSB, MHB and DSCB respectively. The fluid particles are seen entering into the bowl in case of MHB and DSCB. The entry of the fluid particles into the bowl from the squish region and vertical upward orientation of the fluid particles in the bowl counter each other forming a clear vortex motion in these two cases. The establishment of a vortex motion is not very clear in case of HSB. This can be attributed to the relatively low velocities in the Hemi spherical bowl. A similar trend is noticed at 6^0 bTDC (Fig.7) just before the fuel injection in all the three cases. The vortex zones are noticed to intensify further and occupy considerable portion of the bowl in case of DSCB. The shape of DSCB is the main reason for influencing the augmentation and strengthening of the vortex motion.

The fuel is injected at 5.25^0 bTDC, the velocity vector plots at 4^0 bTDC (Fig.8), a little after fuel injection, the velocity vectors near the fuel injector is noticed to be oriented in the direction of the jet. Very high velocities in the range of 110 to 130 m/s are noticed in the fuel jet. The high pressure fuel particles appear to push the fluid molecules in the direction of fuel injection due to the momentum exchange between spray droplets and fluid molecules. At this stage velocity decay occurs in case of MHB and DSCB and this is attributed to large wall friction losses due to the higher surface to volume ratio in these two cases compared to HSB. Minimum velocity 0.0137 m/s is noticed in case of MHB, where as the minimum velocity in case of HSB is 0.044 m/s. However, the increased diffusion due to the vortex motion is resulting in higher turbulence in the case of DSCB. From the plots it can be concluded that the shape of the bowl has a strong influence on the structure of the fluid motion in the piston bowl.

At 10^0 aTDC (Fig.9) the piston already has started moving towards the BDC due to expansion stroke. Fuel injection is assumed to terminate at 2.65^0 aTDC. At this stage the entire fuel has been injected into the combustion chamber. By this time a reverse squish flow (fluid flow from the bowl region to squish region) is noticed in all the three cases. The velocities in all three combustion chambers are noticed to increase considerably. This can be attributed to the combustion related pressure pulses. The vortex formation is strong and occupies major portion of the bowl region in case of DSCB. The magnitude of velocities are appreciably high at the location "⊗" (Ref.Fig.9©). The vortex formation in case of MHB is not as strong as that of DSCB and the location is near the bottom of the bowl. Poor swirling motion in HSB, as noticed from Fig.9(a), can be takes as a cause for poor fuel-air mixing.

At 20^0 aTDC (Fig.10) majority of the fluid in the combustion chamber are the burnt gases. At this stage the velocities noticed in HSB are considerably low as compared to the other two cases. The maximum velocity noticed is 8.9 m/s, whereas, the maximum velocities noticed in case of MHB and DSCB are around 14 m/s. It is noticed that the swirling flow in squish region is strong due to angular momentum movement from bowl region to squish region in case of MHB and DSCB.

7) Comparisions of Pressure Variations with Crank Angle for Different Bowl Configurations:

Fig.11 presents the variation of in-cylinder pressure with crank angle during compression and expansion strokes. The pressure variation is studied from 40^0 bTDC in compression stroke to 80^0 aTDC in expansion stroke. A smooth pressure rise due to compression is noticed from 40^0 bTDC to 5^0 bTDC during compression stroke. The pressure rise is noticed to be same for all the three bowl configurations, as the volume of the piston bowls is the same. During this period the pressure is noticed to increase from 9.87 bar to 45 bar. After the commencement of fuel injection i.e., after 5.25^0 bTDC a slight drop in the in-cylinder pressure is noticed in all three cases. This can be attributed to the fact that the injected fuel evaporates taking energy from the air which results in slight drop in in-cylinder temperature and hence pressure. During the expansion stroke for about 4^0 aTDC the pressure curve is seen to be almost flat indicating pre-flame reaction carrying slight increase in pressure which is nullified by the expansion of gases. At about 7^0 aTDC a rapid rise in pressure is noticed in case of HSB. This can be due to the bulk of the fuel burning.

The peak pressure in this case is noticed to be 82 bar. In case of DSCB the flat portion of the curve is extended up to 12^0 aTDC. This indicates that the bulk of the fuel in combustion chamber has not participated in combustion reaction. A sudden rise in pressure is noticed at 12^0 aTDC indicating the initiation of combustion at multiple locations. The peak pressure is noticed to occur at 16^0 aTDC. The magnitude of peak pressure 68 bar is noticed to be considerably lower to the 82 bar peak pressure in case of HSB. The downward movement of the piston in the expansion stroke counters the pressure rise due to heat release. In case of MHB after TDC continuous drop in pressure is noticed up to 13^0 aTDC. This indicates late combustion (greater ignition delay) in this case. Pressure is 15.85% less in case of DSCB and 18.29 % less in case of MHB compared with HSB.

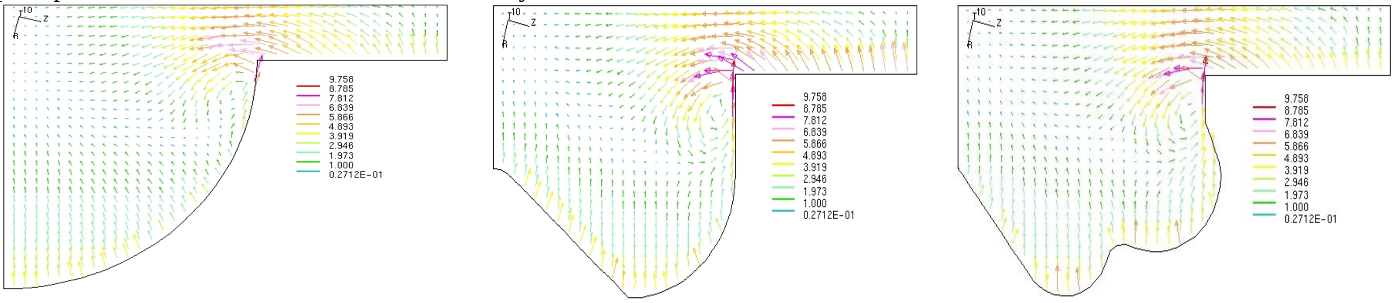

a) Hemispherical Bowl b) Mexican Hat Bowl c) Double Swirl Combustion Bowl

Fig. 6 Velocity Vectors in xz- plane at 20^0 bTDC Crank Angle Position

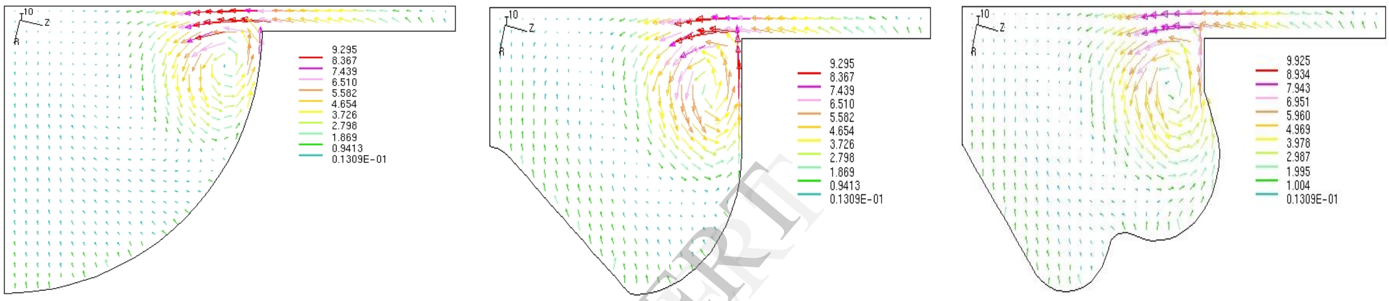

a) Hemispherical Bowl b) Mexican Hat Bowl c) Double Swirl Combustion Bowl

Fig. 7 Velocity Vectors in xz- plane at 6^0 bTDC Crank Angle Position

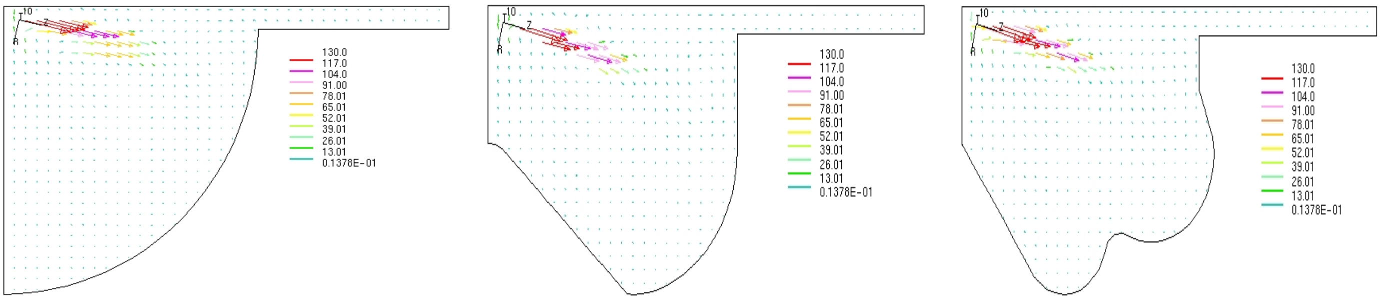

a) Hemispherical Bowl b) Mexican Hat Bowl c) Double Swirl Combustion Bowl

Fig. 8 Velocity Vectors in xz- plane at 4^0 bTDC Crank Angle Position

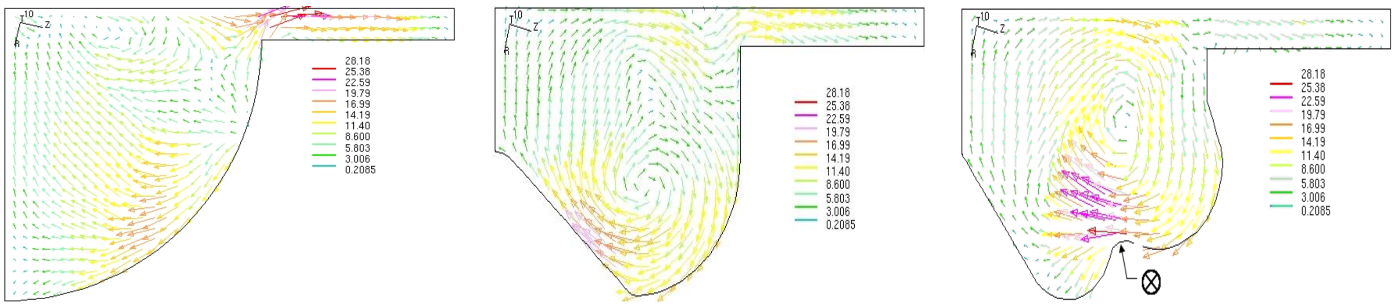

a) Hemispherical Bowl b) Mexican Hat Bowl c) Double Swirl Combustion Bowl

Fig. 9 Velocity Vectors in xz- plane at 10^0 aTDC Crank Angle Position

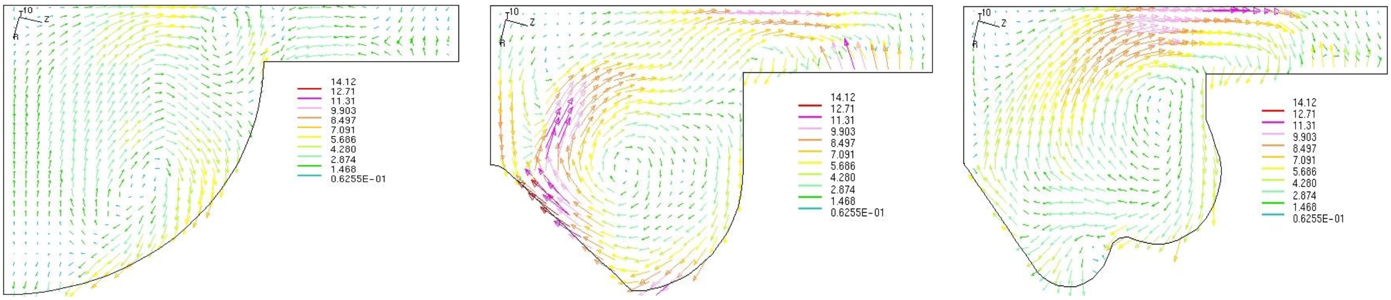

a) Hemispherical Bowl b) Mexican Hat Bowl c) Double Swirl Combustion Bowl

Fig. 10 Velocity Vectors in xz- plane at 20^0 aTDC Crank Angle Position

8) Comparison of Turbulent Kinetic Energy Variation with Crank Angle for Different Bowl Configurations:

Fig.12 presents the average Turbulent Kinetic Energy (TKE) Vs crank angle plots for HSB, MHB and DSCB cases. From the figure it is observed that TKE levels are slightly low in case of HSB and MHB till the time of fuel injection. During this period the TKE is noticed to be higher, in case of DSCB due to the stronger swirl effects. A sharp rise in turbulent kinetic energy is noticed in all the three cases, with the commencement of fuel injection. The peak TKE's is noticed to occur at around 4^0 aTDC, the peak values estimated from Fig. 12 are 45, 47 and 31 m^2/s^2 for HSB, DSCB and MHB. Sharp fall in TKE is noticed after the completion of fuel injection as the piston started moving down during the expansion stroke. Interestingly a sudden rise in the TKE plots is noticed at 9^0 aTDC for HSB, 12^0 aTDC for DSCB and 16^0 aTDC for MHB. These bumps indicate the increase in turbulent kinetic energy due to initiation of combustion. From the end of fuel injection to 40^0 aTDC the TKE of DSCB is noticed to be higher than the TKE's of the other two bowls. The fluid motion during the period greatly affects the fuel-air mixing and combustion. Higher TKE in case of DSCB indicate that the bowl shape augments compression swirl. From 40^0 aTDC onwards the TKE of the three bowls behave similar. The TKE is 37.78 % less in case of MHB compared with HSB and DSCB.

9) Comparision of Swirl Ratio Variations with Crank Angle for Different Bowl Configurtions:

Fig. 13, 14 and 15 presents the squish, swirl and tumble ratios Vs crank angle plots for different bowl configurations in x, y and z axis respectively. These ratios depends on angular momentum of fluid which is influenced by bowl shape, fuel injection velocity, direction of fuel injection, combustion of fuel also influence the flow direction and velocity of fluid inside the combustion chamber. The squish ratios Vs crank angle plots (Fig 13) indicate the compression squish is more or less same for MHB and DSCB until the piston reaches TDC. The bowl shape has a direct influence on squish ratio during this period. The squish ratio is noticed to be lower by 0.6 in case of HSB. The initiation of the combustion appears to affect the squish ratios due to the sudden expansion of gases in the combustion zones. These are noticed at 9^0 aTDC for HSB, 12^0 aTDC for DSCB and 16^0 aTDC for MHB. The rise in squish ratio is noticed to be very sharp in case of HSB due to reverse squish flows causing the sharp increase. At about 11^0 aTDC the squish ratios for the three bowls are noticed to be the same. In case of MHB and DSCB, from 30^0 aTDC the squish ratios are falling due to the increase in the combustion chamber volume during the expansion stroke. In case of HSB the squish ratio is increasing even after 20^0 aTDC this can be attributed due to late combustion of considerable part of the fuel in this case (combustion in case of HSB is highly heterogeneous as discussed in velocity vector plots and temperature contours). The squish ratio is falling very sharply in the later part of the expansion stroke in HSB as bowl shape is not supporting the squish.

The swirl ratio in y-axis (Fig.14) observed to follow similar trend in case of MHB and DSCB up to the start of fuel injection, where as in case of HSB it is different and the swirl ratio is observed to be low compared to MHB and DSCB up to the start of fuel injection. The high swirl ratio is observed in case of HSB i.e. 4.0 (during the period of combustion) where as in case of MHB it is 2.5 and in DSCB it is 3.5. A sudden drop in swirl ratios is noticed immediately after the combustion due to the increase in the combustion chamber volume. A sharp fall in the y-axis swirl ratio is observed from 2.5 to 0.9 during 16^0 aTDC and 18^0 aTDC. Delayed combustion (as late as 16^0 aTDC) appears to be the reason for the sudden drop in the angular momentum. In case of DSCB the swirl ratio is increased up to 5^0 aTDC and the swirl ratio is observed 3.2 at 5^0 aTDC higher than that of MHB indicate the suitability of DSC Bowl shape in the swirl point of view.

The tumble ratio in z-axis (tumble ratio) is observed from the Fig.15 for different bowl configurations and it is constant up to the fuel injection in all the cases. But the tumble ratio before fuel injection in case of HSB is 2.9 and in case of MHB and DSCB it is 1.4 this is because low squish effect in case of HSB. The high pressure fuel jet, combustion chamber volume affects the tumble ratio.

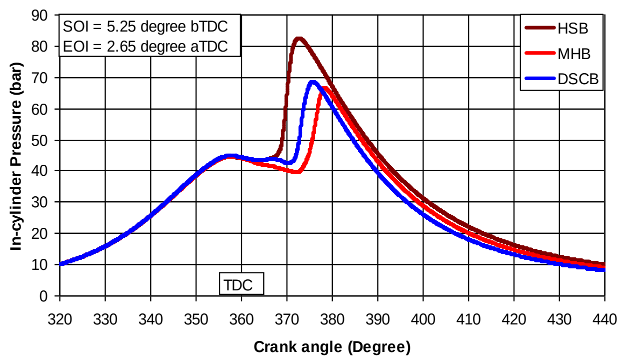

Fig.11 Effect of Bowl Configuration on Volume-Averaged In-Cylinder Pressure

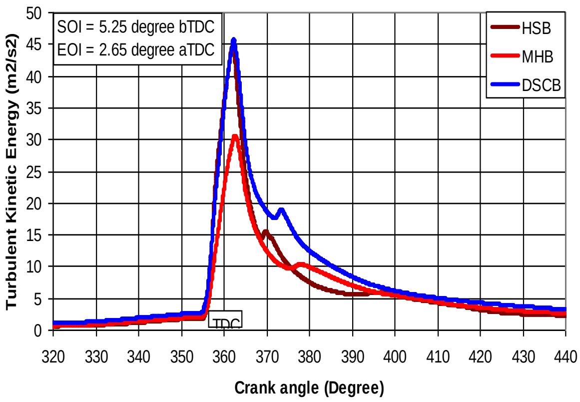

Fig.12 Effect of Bowl Configuration on Volume-Averaged Turbulent Kinetic Energy

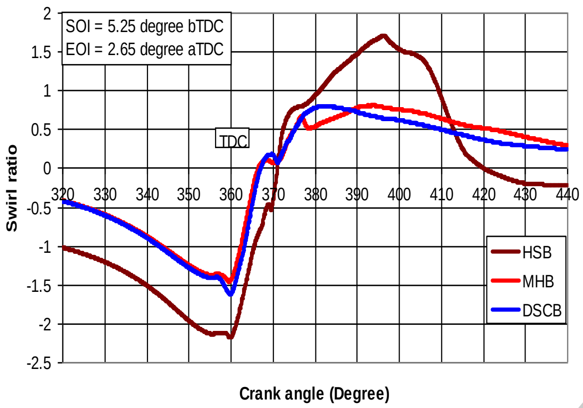

Fig.13 Effect of Bowl Configuration on Swirl ration in X-direction

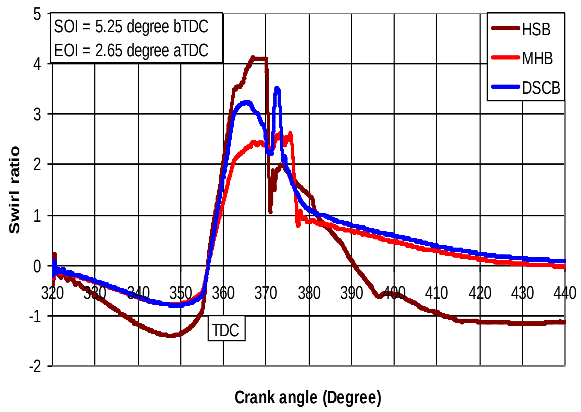

Fig.14 Effect of Bowl Configuration on Swirl Ratio in Y-direction

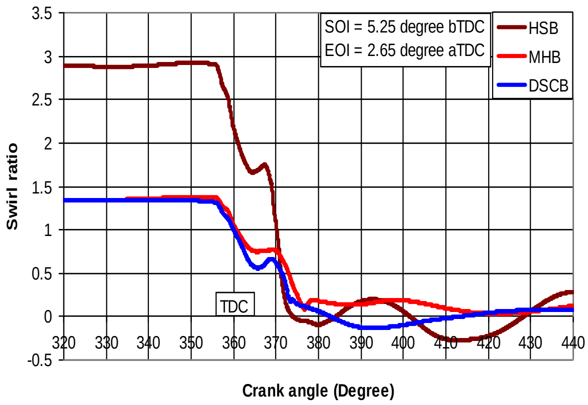

Fig15. Effect of Bowl Configuration on Swirl Ratio in Z-direction

VIII. CONCLUSIONS

From the above work it is concluded that the Double swirl combustion bowl (DSCB) is the best among the three bowl configurations (Hemispherical bowl, Mexican hat bowl and Double swirl combustion bowl). That is why In-cylinder pressure is 15.85% less in case of DSCB and 18.29 % less in case of MHB when compared with HSB. The TKE is 37.78 % less in case of MHB compared with HSB and DSCB. Based on the above facts and figures it is concluded that the Double Swirl Combustion Chamber is the best for the engine under consideration.

REFERENCES

[1] M. E. McCracken and J. Abraham,"Swirl-Spray Interactions in a Diesel Engine". SAE Technical Paper. 2001-01-0996.

[2] Rahman M. Montajir, H. Tsunemoto and H. Ishitani., “Fuel Spray Behavior in a Small DI Diesel Engine: Effect of Combustion Chamber Geometry”. SAE Technical Paper. 2000-01-0946.

[3] G.M. Bianchi and P. Pelloni, "Modeling the Diesel Fuel Spray Breakup by Using a Hybrid Model", SAE Technical Paper.1999-01-0226.

[4] Yoshiyuki Kidoguchi, Changlin Yang and Kei Miwa, "Effect of High Squish Combustion Chamber on Simultaneous Reduction of NOx and Particulate from a Direct-Injection Diesel Engine", SAE Technical Paper. 1999-01-1502.

[5] Sung, N.W., Choi, J.S. and Jeong, Y.I., “A Study on the Flow in the Engine Intake System” SAE Paper No. 952067, 1995.

[6] Alex B.Liu, Daniel Mather and Rolf D. Reitz, “Modelling the Effects of Drop Drag and Up Fuel Sprays”, SAE Paper No. 930072, 1993.

[7] Tree, D. R., and Foster, D. E. "Optical Soot Particle-Size and Number Density-Measurements in a Direct-Injection Diesel-Engine", Combust. Sci. Technol., 95, 313-331, 1994.